Respiratory failure triggered by cholinesterase inhibitors may involve activation of a reflex sensory pathway by acetylcholine spillover

Aurélie Nervo, André-Guilhem Calas, Florian Nachon, Eric Krejci

Title: Respiratory failure triggered by cholinesterase inhibitors may involve activation of a reflex sensory pathway by acetylcholine spillover

Authors: Aurélie Nervo, André-Guilhem Calas, Florian Nachon, Eric Krejci

PII: S0300-483X(19)30169-6
DOI: https://doi.org/10.1016/j.tox.2019.06.003
Reference: TOX 52232

To appear in: *Toxicology*

Received date: 21 March 2019
Revised date: 15 May 2019
Accepted date: 5 June 2019

Please cite this article as: Nervo A, Calas A-Guilhem, Nachon F, Krejci E, Respiratory failure triggered by cholinesterase inhibitors may involve activation of a reflex sensory pathway by acetylcholine spillover, *Toxicology* (2019), https://doi.org/10.1016/j.tox.2019.06.003

Respiratory failure triggered by cholinesterase inhibitors may involve activation of a reflex sensory pathway by acetylcholine spillover

Aurélie Nervo[1, 2], André-Guilhem Calas[1, 2], Florian Nachon[1], Eric Krejci[2]

[1]Département de Toxicologie et Risques Chimiques, Institut de Recherche Biomédicale des Armées, Brétigny-sur-Orge, France

[2]COGnition and Action Group, UMR 8257, CNRS, Université Paris Descartes, Paris, France

corresponding author: eric.krejci@parisdescartes.fr

Graphical abstract

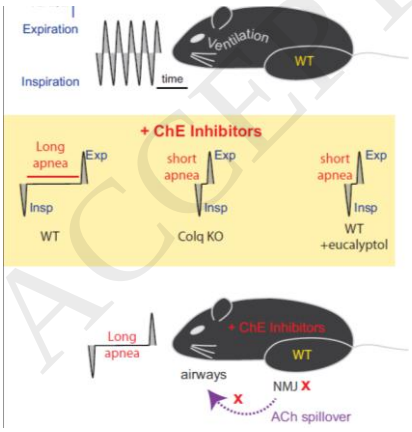

Highlights (3 à 5 de 125 caractères max avec les espaces)

- Inhibition of cholinesterase by organophosphate poisoning strongly impacts respiration patterns.
- Long pauses after inspiration are mainly triggered by brain-permeant cholinesterase inhibitors.
- Mutant mice with normal acetylcholinesterase in brain and deficient in muscles do not present long pauses post-inspiration after brain-permeant inhibitors exposure.
- Long pauses after inspiration caused by nasal irritants are reversed by eucalyptol acting on afferent sensory neurons, presumably by acting TRPM8 receptor.
- Long pauses after inspiration triggered by brain permeant cholinesterase inhibitors are reversed by eucalyptol.

Abstract

Respiration failure during exposure by cholinesterase inhibitors has been widely assumed to be due to inhibition of cholinesterase in the brain. Using a double chamber plethysmograph to measure various respiratory parameters, we observed long “end inspiratory pauses” (EIP) during most exposure that depressed breathing. Surprisingly, Colq KO mice that have a normal level of acetylcholinesterase (AChE) in the brain but a severe deficit in muscles and other peripheral tissues do not pause the breathing by long EIP. In mice, long EIP can be triggered by a nasal irritant. Eucalyptol, an agonist of cold receptor (TRPM8) acting on afferent sensory neurons and known to reduce the EIP triggered by such irritants, strongly reduced the EIP induced by cholinesterase inhibitor. These results suggest that acetylcholine

(ACh) spillover from the neuromuscular junction , which is unchanged in Colq KO mice, may activate afferent sensory systems and trigger sensory reflexes, as reversed by eucalyptol. Indeed, the role of AChE at the cholinergic synapses is not only to accurately control the synaptic transmission but also to prevent the spillover of ACh. In the peripheral tissues, the ACh flood induced by cholinesterase inhibition may be very toxic due to interaction with non-neuronal cells that use ACh at low levels to communicate with afferent sensory neurons.

keywords (max 6)

acetylcholinesterase; butyrylcholinesterase; organophosphate; respiration; mice; eucalyptol

1 Introduction

According to the EMA (European Medical Agency) (2003), treating respiratory failure by controlled ventilation after intubation is the immediate therapeutic priority after poisoning by acute doses of organophosphate compounds (OP) (Stone, 2018a). OP and carbamates contribute to pesticide exposure with around 100,000 deaths/year worldwide (Eddleston, 2019). OP chemical warfare nerve agents, such as sarin, have intoxicated people during the Iran-Iraq war (midd-1980) (Stone, 2018a), and in Syria (2013, 2017) (Dolgin, 2013). Indeed, even low doses and short exposure to these irreversible inhibitors of acetylcholinesterase (AChE) and butyrylcholinesterase (BChE) induced subsequent, well-characterized cholinergic syndrome including miosis, seizures, and apnea (Cannard, 2006), and finally death. Thus, deaths following acute OP exposure are due to respiratory failure. In addition to this

toxidrome, OP affect others system in a time dependent manners, such as neurogenic inflammation, immune-neuro interaction and oxidative stress leading to airway hyperreactivity (Shaffo et al., 2018).

The current scientific paradigm explaining the respiratory failure caused by OP poisoning is focused nearly exclusively on cholinergic synaptic transmission consequences of these chemicals. It is assumed that after cholinesterase (ChE) inhibition the excess of acetylcholine (ACh) in the central cholinergic synapses dramatically affects the respiratory centers in the central nervous system (CNS) and leads to the respiratory arrest by central apnea (Hulse et al., 2014; Stone, 2018b).

However, this paradigm does not fully agree with observations in AChE knockout (KO) mice that need special care during the post-natal development (Duysen et al., 2002) but they can survive into adulthood, likely because BChE acts as a back-up enzyme for deficient AChE (Hartmann et al., 2007). The surviving AChE KO mice are very sensitive to OPs and to selective BChE inhibitors as bambuterol (Duysen et al., 2001; Xie et al., 2000): adult and neonate AChE KO mice stop breathing following peripheral blockade of BChE. Since this selective BChE inhibitor used does not reach BChE in the CNS, and since it does not perturb central respiratory activity recorded from spinal nerve rootlets in the brainstem of AChE KO mice (Chatonnet et al., 2003), these observations suggest that in AChE KO mice OPs and this selective BChE inhibitor act on peripheral ChEs. A plausible target is the neuromuscular junction (NMJ) where BChE, is anchored on the terminal Schwann cells and control ACh spillover (Petrov et al., 2014). However, in AChE KO mice, BChE inhibitors do not change the amplitude of repetitive end plate potential (EPP) triggered by nerve stimulation at different frequency (Minic et al., 2003). Thus, the ventilation failure after inhibition of BChE

cannot be caused by an acute failure of muscle contraction resulting from the reduction of the amplitude of the EPP below a threshold to generate muscle action potential.

We decided to extend the observations made on AChE KO mice by examining the effects of cholinesterase inhibitors (ChEIs) on mice having a partial deficit of AChE. We selected three lines: two in which AChE anchoring is deficient (PRiMA KO and Colq KO mice) and one in which AChE is not expressed in skeletal muscles (AChE1iRR). PRiMA is the main anchor of AChE in the CNS, where it anchors AChE tetramers at the plasma membrane in cholinergic neurons (Dobbertin et al., 2009). PRiMA KO mice have practically no AChE in the brain and yet adapt remarkably to the resulting excess of ACh in brain (Farar et al., 2012). They have normal AChE level at the NMJ (Bernard et al., 2011) and breathe normally (Boudinot et al., 2009). Colq protein clusters AChE at the NMJ (Bernard et al., 2011). Colq KO mice present a severe growth retardation and muscle weakness (Bernard et al., 2011; Feng et al., 1999). Finally, AChE1iRR mice, in which a short deletion in intron 1 prevents the expression of AChE in skeletal muscles and in derivative neural crest cells (Bernard et al., 2011; Camp et al., 2010), also show muscle weakness but do not have the severe growth retardation of Colq KO mice and breathe normally (Boudinot et al., 2009).

To evaluate the respiratory effects of ChEIs in WT mice and in AChE deficient mice, we recorded nasal and thoracic flows separately by double chamber plethysmography (DCP), measured respiratory frequency, identified apneic episodes, and measured specific airway resistance. To inhibit ChEs we selected sub-lethal doses of paraoxon, an OP pesticide metabolite that crosses the blood brain barrier (BBB); physostigmine, a carbamate that crosses the BBB; and pyridostigmine, a carbamate that does not cross the BBB. We showed that respiratory changes were induced by not only AChE inhibition in the brain but also by the

inhibition of peripheral ChEs. In particular, long pauses after inspiration (called end inspiratory pauses, EIP), a classical and stereotyped respiratory reflexe to irritant molecules exposure, were observed after mice exposure and could not be simply explained by AChE inhibition at cholinergic synapses in the brain nor at the NMJ alone. Since the duration of EIP observed when mice breathe irritant molecules can be reduced by eucalyptol, we tested the effects of this compound on EIP triggered by physostigmine.

2 Materials and methods

2.1 Animals

Adult male and female mice were maintained on a mixed B6D2 genetic background. Before beginning any experiment, they were housed for 7 days, in an environment maintained at 23 ± 0.5°C, 38-41% of humidity, on a 12h dark/light cycle with light provided between 7a.m and 7p.m. They were given food and water *ad libitum*. All experiments were carried out in compliance with the European Committees Council Directive (86/609/EEC) and were approved by Paris Descartes University ethics committee for animal experimentation (CEEA34.EK/AGC/LB.111.12).

Experiments were performed on four strains of mice: (1) Wild type (WT) mice (n=45) were picked in the colonies in which Colq KO and AChE1iRR KO mice were maintained as heterozygotes, (2) PRiMA KO mice (n=25) have an inactivation of exon 3 encoding the domain that interacts with AChE (Dobbertin et al., 2009). (3) Colq KO mice (n=16) have a deletion of the exon2 encoding the domain that interacts with AChE (Feng et al., 1999). (4) *AChE1iRR* mice (n=16) have a deletion of an enhanceosome in intron1 of AChE gene which

prevent the expression of AChE in skeletal muscles and in cells deriving from the neural crest (Camp et al., 2008).

2.2 Chemicals

Each compound was injected as 10µL of solution per 1g of mouse body weight subcutaneously (s.c). The injected solutions were prepared daily. Sub-lethal doses of ChEI have been adequately chosen to induce quantifiable respiratory modifications.

-Saline solution (0.9% NaCl) + dimethyl sulfoxide (DMSO) 1% was used as control (vehicle).

-Paraoxon was purchased from Sigma-Aldrich® (Saint-Quentin Fallavier, France), CAS 311-45-5. The solution was stocked at a concentration of 35mg/mL into DMSO at 4°C. The stock solution was dissolved at 0.4mg/kg into saline solution.

-Physostigmine hemisulfate was purchased from Santa Cruz Biotechnology® (Dallas, Texas), CAS 64-47-1. The solution was stocked at a concentration of 0.001mol/L into saline solution. The stock solution was dissolved at 0.27mg/kg into saline solution.

-Pyridostigmine bromide (3-dimethylaminocarbonyloxy-N-methylpyridinium bromide) was purchased from Sigma-Aldrich® (Saint-Quentin Fallavier, France), CAS 101-26-8. The solution was stocked at a concentration of 0.01mol/L into physiological saline. The stock solution was then dissolved at 1.65mg/kg into saline solution.

-Eucalyptol (1,8-cineaole), a TRPM8 (transient receptor potential cation channel subfamily M member 8) agonist involved in the sensory system and in mediating analgesia, was purchased from Sigma-Aldrich® (Saint-Quentin Fallavier, France), CAS 470-82-6. The efficient dose was estimated at 300mg/kg (Ha et al., 2015). A total volume of 20µL of eucalyptol diluted in

corn oil was instilled intranasally, drop by drop alternatively in each nostril using a positive-displacement pipet. Two instillations were performed: the first one 7 min before and the second one 13 min after subcutaneous injection of ChEIs.The duration of instillation was around 2 minutes.

2.3 Double chamber plethysmography

We used the double-chamber plethysmograph (DCP) (Emka Technologies®, Paris, France) to follow the ventilation (Hoymann, 2012). The plethysmograph contains two chambers: a head chamber and a body chamber. The mouse is placed in a conical restrainer which follows the animal's head shape and ensures that there is no airflow between the two chambers. The conical restrainer is inserted into the body chamber. The plethysmograph has two pneumotachographs (pnt). These are air passages which establish a linear relationship between airflow and pressure difference on each side. The pressure depends on the breathing of the mouse. The breathing creates two distinct airflows: the nasal flow, generated by flow of air in and out of the nose; and the thoracic flow, generated by compression and expansion of air when the thorax rises and falls. The two flows are recorded in parallel at a frequency of 2000Hz. The changes of pressure in each compartment are measured, independently of temperature, by a differential pressure transducer (dpt). One dpt measures the pressure difference between the head chamber and the atmosphere. The other dpt measures the pressure difference between the body chamber and the atmosphere (Fig 1A). This non-invasive technique, used in conscious mice, avoids the need of anesthesia.

2.3.1 Analyzers setting

The analyzers measure the time delay between the nasal and thoracic flow that depends on airway resistance. Each analyzer is tuned as follow:

- flow threshold: 0.15mL/s
- measure RT at: 30% of tidal volume (TV)
- start inspiration interpolate from: 5% peak inspiratory flow (PIF)
- compute breathing rate from: peak expiration flow (PEF) to peak inspiratory flow (PIF)
- end inspiratory pause (EIP): interpolation of 60% PEF
- end expiratory pause (EEP): interpolation of 30% PEF

2.3.2 Recording

Naïve mice were inserted in the tube 5 minutes before recording to acclimate them to the device. The physiological breathing was recorded over 15 minutes as an internal control. Then, the mouse was taken out of the DCP. Depending on its group, the mouse received a subcutaneous injection and/or a nasal instillation of the compounds. Then, the breathing was recorded for 35 minutes. The clinical symptoms of poisoning were only visible when the mouse came out of the tube. They were thus noted at the end of each experiment. The mice which had been challenged with toxic compounds were euthanized by an overdose of pentobarbital dissolved into saline solution.

2.4 Data analysis

2.4.1 Groups of mice

The mice strains have been challenged randomly with toxic compounds. Distribution of mice in terms of body weight, age and number in each group combining strain and compound is detailed in table S1.

2.4.2 Parameters setting

The raw data of the breathing were visualized and analyzed manually using LabChart Pro V8® (ADInstruments©, Paris, France) and automatically by Iox® (Emka Technologies software®, Paris, France). In LabChart the peak inspiratory flow was selected to define the beginning of each breathing cycle since it was an easy and reliable parameter. We calculated, for each cycle, the other parameters for the nasal and thoracic flow: respiratory frequency, tidal volume, peak inspiratory flow, peak expiratory flow and amplitude. Each parameter was averaged over a window of 5 seconds, selected approximately every 20 seconds. In Iox®, inspiratory time, expiratory time, end inspiratory pause, end expiratory pause, time delay, specific airway resistance and volume minute were determined automatically for each cycle. They were determined as illustrated in supplementary figure:

-Ti (time of inspiration) started at the intersection of the straight line defined by the point 5% and 10% of PIF and the line of flow 0 and finished at the intersection of the straight line defined by the point 10% and 5% of PIF and the line of flow 0.

-EIP (End inspiratory pause) were included into Te. EIP started at the end of the inspiration period and ended at the intersection of the straight line defined by the point 40% and 80% of PEF and the line of flow 0.

-sR_{AW} (specific airways resistance) was calculated according to a mathematical formula previously described (Pennock et al., 1979).

2.4.3 Intra-group comparison

Data were evaluated using OriginPro® (OriginLab, Northampton, MA). All parameters obtained with LabChart Pro V8® or Iox® were represented over time for each mouse. We compared the recorded parameters of breathing between 0 and 14min30s (corresponding to physiological breathing, called “before” in figures) (n=±30 sequences per mouse) and the ones recorded between 28 and 45min or 33 and 50min (corresponding to altered breathing called “after” in figures) (n±60 sequences per mouse) depending on the time of injection (15 or 20min respectively after the introduction of both mice in their restrainer).

We obtained, for each parameter, the mean value ± standard deviation for each mouse, before and after injection of the compound. To filter the values given by Iox® due to the mouse moving or signal distortion, we selected Iox® data according to the mean of respiratory frequency ± standard deviation obtained and validated by selection of raw data in Labchart® (the sequence of 5 seconds was validated if and only if the respiratory frequency of the thorax was equal of the respiratory frequency of the nasal ±0.5 Hz)

To compare each parameter, we used a paired sample t-Test of the mean values between the physiological (before injection) and the altered (after injection) breathing. In the figures, data

(respiratory frequency, Ti, EIP and sR_{AW}) were represented in box charts (with percentiles 25 and 75). *P*-values of less than 0.05 were considered as significant.

2.4.4 Inter-group comparison

Data were evaluated using OriginPro® software. All parameters obtained, with LabChart® or Iox®, were represented over time for each mouse. According to the administered compound or the genetic background of the mouse, the recorded parameters of breathing between 28 and 45min or 33 and 50min (altered breathing=after) (n±60 per mouse), depending on the time of injection (15 or 20min), were compared using a one-way ANOVA followed by Tukey *posthoc* test. We chose to represent the absolute value and the percentage of the variation of each parameter from their physiological value. In the figures, data (respiratory frequency, Ti, EIP and sR_{AW}) were represented in box charts (with percentiles 25 and 75). *P*-values of less than 0.05 were considered as significant.

Statistical analysis was done, on the mean value (intra and inter-group) of each parameter and as well as on the percentage of variation (inter-group) of each parameter. The latter value allowed determining the trend of the variation before and after injection of compound and to compare the value between groups. However, EIP has not been represented in percentage of variation because its values before injection was less than 1ms; which implied that the variations of the values for these data were too heterogeneous and could not be used to draw any meaningful conclusion.

The variation of the volume exchanged has been observed on the absolute mean values.

The mean value of some parameters (Fq, Ti, Te, EIP, EEP, RT, MV: the volume of gas inhaled (inhaled minute volume) and exhaled (exhaled minute volume) from the lungs of a

mouse per minute were also represented for each group in order to compare the evolution of breathing over time.

3 Results

3.1 At rest, mice with a severe deficit of synaptic AChE breathed almost normally

Double chamber plethysmography is a sensitive method to simultaneously quantify the flow of air that passes through the nose and the flow of air moved by the thorax during the breathing cycle (Fig 1A). We have compared the breathing ventilation of WT mice with that of the mice in which AChE is not anchored on CNS cholinergic neurons (PRiMA KO mice) or absent at the NMJ (AChE1iRR and Colq KO mice). A representative example of the airflow is presented in (Fig 1B) for WT and mutant mice. WT mice breathed with an average respiratory frequency of 304±27 cycles per minute (cpm). There was no significant difference between WT mice and mutant mice: the mean respiratory frequency of PRiMA KO mice was 303±57cpm ($p>0.05$), that of AChE1iRR mice was 296±59cpm ($p>0.05$), and that of Colq KO mice was 248±37cpm ($p>0.05$). Other parameters like the inspiratory time, the expiratory time and the thoracic tidal volume were similar in the four mouse strains (Fig 1C and S2 Table). The Colq KO mice differed from the other mice strains by the higher specific airway resistance (5.3±1cm H_2O.s) than in WT (4.0±0.5cm H_2O.s, $p<0.05$) and in PRiMA KO (3.8±1cm H_2O.s, $p<0.01$) mice. The mice with AChE deficits at the NMJ tend to have an affected pattern (dynamic of airflow during inspiration phase), but that it did not affect the basic physiology of breathing, indicating adequate adaptation of cholinergic synapses in the muscles. Despite the fine control of airflow was changed in mice with AChE deficit at the NMJ, we did not observe any major difference of breathing parameters between the mutant

mice and the WT mice (S2 Table). We concluded that all the mutant mice adapt remarkably to the deficit of AChE in cholinergic synapses of CNS or skeletal muscles.

3.2 In WT mice both paraoxon and physostigmine changed breathing pattern more severely than pyridostigmine

In WT mice, acute intoxications with 0.4mg/kg of paraoxon or 0.27mg/kg of physostigmine both dramatically changed their breathing pattern (Fig 2A and 2B). The respiratory frequency decreased by 64% (295±41cpm to 112±85cpm, $p<0.01$) after paraoxon and by 78% (283±42cpm to 61±16cpm, $p<0.01$) after physostigmine. The decrease of the respiratory frequency was similar between both groups ($p>0.05$). The mean values of the respiratory frequency were both significantly lower than those of the control group injected with vehicle ($p<0.01$ for both paraoxon and physostigmine) (Fig 2C). The frequency reduction was partly due to a significant increase in inspiratory time (72%: from 97±11ms to 169±55ms, $p<0.01$ for paraoxon and 97% from 103±16ms to 200±17ms, $p<0.01$ for physostigmine) but mainly due to an increase of 430% in the expiratory time (112±15ms to 617±339ms, $p<0.01$) after paraoxon and by 668% (114±22ms to 863±292ms, $p<0.01$) after physostigmine. The increase of the inspiratory and expiratory time was similar in each group ($p>0.05$ for both) whereas the mean values of the inspiratory and expiratory time were significantly higher than those of the group injected with vehicle ($p<0.01$ for both paraoxon and physostigmine) (S2 Table). The increase of expiratory time (data not shown) was mostly due to the appearance of EIP of variable duration: from 3±2ms to 322±225ms ($p<0.01$) after paraoxon and from 15±9ms to 672±265ms, ($p<0.01$) after physostigmine. EIP after physostigmine were longer than the ones obtained after paraoxon ($p<0.01$) (Fig 2C). The specific airways resistance was increased after

pyridostigmine poisoning compared to vehicle ($p<0.001$), paraoxon ($p<0,01$) and physostigmine ($p<0,01$) injection.

A classical pharmacological strategy to distinguish central versus peripheral action of ChEIs is to compare the action of membrane permeant inhibitors, like physostigmine, with the action of charged inhibitors like pyridostigmine that cannot cross the BBB and therefore cannot reach the brain ChEs. We thus exposed WT mice to pyridostigmine. Mice treated with a sub-lethal dose of pyridostigmine (1.65mg/kg) presented smaller alterations of breathing than WT mice exposed to physostigmine (Fig 2). The respiratory frequency was decreased but less than with physostigmine ($p<0.01$) and there were no EIP ($p>0.05$). The resistance of airways was increased by 82% (3.8±0.7 to 6.8±1.2cm H_2O.s, $p<0.01$) (S2 Table). The profile of ventilation after pyridostigmine exposure is thus significantly different than that observed with physostigmine or paraoxon.

3.3 PRiMA KO mice have more similar sensitivity to physostigmine and pyridostigmine than WT mice

To explore if the difference of response to physostigmine and pyridostigmine resulted from the selective inhibition of brain AChE by physostigmine, we exposed PRiMA KO mice that are adapted to the absence of central AChE and to the resulting high level of ACh in CNS (Farar et al., 2012). We expected that physostigmine would only minimally change the respiration in PRiMA KO mice, and would mimic the effects of pyridostigmine on WT mice. However, as illustrated (Fig 3A and 3B), the respiration of PRiMA KO mice was significantly changed by physostigmine or pyridostigmine and presented a similar reduction of respiratory frequency ($p>0.05$): from 303±48cpm to 132±35cpm, ($p<0.01$) for physostigmine and from 310±60cpm to 171±24cpm, ($p<0.01$) for pyridostigmine (Fig 3B). Physostigmine and

pyridostigmine both induced a similar increase of Ti ($p>0.05$) (Fig 3C). As in WT mice, pyridostigmine triggered only very short EIP (5±6ms to 38±25ms, $p=0.025$). Physostigmine triggered EIP (12±10ms to 156±136ms, $p<0.05$) (Fig 3C). Despite the differences in the induction of EIP, pyridostigmine and physostigmine produced significant respiratory effects in PRiMA KO mice which have no AChE in the central cholinergic synapses. These effects must therefore have involved the inhibition of peripheral ChEs.

3.4 The depression of ventilation by physostigmine is reduced in Colq KO mice, which have a normal level of AChE in brain

If AChE inhibited by physostigmine in the respiratory center is the main cause of the long EIP in WT mice, we expected the occurrence of long pauses in exposed Colq KO mice in which AChE was normally expressed in the brain. To test this hypothesis, we exposed Colq KO mice to physostigmine (Fig 4A and 4B). The respiratory frequency decreased by 52±10% ($p<0.01$), a decrease which was significant but smaller ($p<0.01$) than that induced by physostigmine in WT mice which was decreased by 79±5% ($p<0.01$) (Fig 4C). Ti increased by 31±23% ($p<0.01$) in Colq KO mice, much less than in WT mice (97±26%, $p<0.01$). More importantly, EIP duration increased 10-fold less in Colq KO mice (64±39ms, $p<0.05$) than in WT mice (672±265ms, $p<0.01$) (Fig 4C). The specific airways resistance, which was higher in control Colq KO mice than in control WT mice ($p<0.05$), was not changed by physostigmine ($p>0.05$). These results supported that the duration of EIP depends significantly on ChE inhibition in peripheral tissues.

3.5 AChE1iRR mice, that do not produce AChE in skeletal muscles react similarly to physostigmine and pyridostigmine

The fact that Colq KO mice were less sensitive to physostigmine than WT mice suggested that the AChE anchored in the NMJ plays a major role in the respiratory failure induced by ChE inhibitors. To further confirm the importance of AChE in skeletal muscles, we examined the breathing of AChE1iRR mice. Despite adapations of the skeletal muscles to the absence of AChE, AChE1iRR mice remained sensitive to physostigmine or pyridostigmine (Fig 5A and 5B). After physostigmine or pyridostigmine injection, the respiratory frequency of these mice decreased respectively by 66±17% ($p<0.01$) and by 44±11% ($p<0.01$) and Te increased respectively by 395±237% ($p<0.01$) and by 119±50% ($p<0.01$). We observed an increase of EIP durations after physostigmine poisoning (21±15ms to 150±77ms, $p<0.01$). As in WT mice; EIP durations increase slightly after pyridostigmine injection (10±7ms to 40±22ms, $p<0.01$). The airways resistance increased respectively by 26±23% ($p<0.05$) and by 59±35% ($p<0.01$) (Fig 5C).

3.6 Eucalyptol shortens the long end inspiratory pause triggered by physostigmine

EIP are stereotyped responses when mice breathe irritant molecules (Dutschmann et al., 2014). Moreover, the duration of EIP triggered by irritant molecules (e.g. acrolein, cyclohexanone, etc) acting on afferent sensory neuron was reduced by menthol or eucalyptol through the activation of TRPM8 (cold and menthol receptor 1) located in afferent neurons (Ha et al., 2015). If EIP triggered by physostigmine have a similar origin (activation of afferent sensory neurons), the duration of EIP could be shortened by eucalyptol.

Eucalyptol instilled alone did not change overall breathing parameters (data not shown). Instillations of eucalyptol before and after injection of physostigmine reduced the duration of EIP by 10-fold from 672±265ms (without eucalyptol) to 67±50ms (with eucalyptol) ($p<0.01$) (Fig 6C). However, eucalyptol treatment slightly rescued the respiratory frequency decreased provoked by physostigmine poisoning ($p<0.05$) and did not reduce Ti (S2 Table). The instillation of eucalyptol increased the airways resistance. Indeed, sR_{AW} value of the group treated with eucalyptol alone increased by 9% (3.7±0.3 to 3.9±0.2cm H_2O.s, $p<0.05$). It was exacerbated ($p<0.01$) in mice exposed to physostigmine and treated by eucalyptol, with a significant increase of 122% (3.5±0.4 to 8.0±3.7cm H_2O.s, $p<0.01$) compared to the group with physostigmine alone, which did not present any increase of sR_{AW} (3.9±1.3 to 4.9±1.2cm H_2O.s, $p>0.05$) (Fig 6C).

4 Discussion

The respiratory failures triggered by OPs are multifactorial due to the fact that these very reactive molecules bind diverse proteins in addition to ChE. However, it strikingly resembles the syndrome induced by carbamate pesticides (Hulse et al., 2014), which are more selective inhibitors of ChEs. One can thus assume that ChE inhibition is responsible for the respiratory failure for both classes of compounds. ChEs are present both in the CNS and in the peripheral nervous system (PNS). We have taken advantage of mice in which AChE is absent in the synapses either in the CNS or in the PNS to evaluate the relative contributions of the inhibition of central and peripheral ChEs to specific respiratory pauses, the pause after inspiration that were specifically triggered by physostigmine and paraoxon but not by pyridostigmine. We exposed mice to ChEIs in which AChE is either not anchored in

cholinergic synapses in the CNS (PRiMA KO mice) or absent at the NMJ (Colq KO or AChE1iRR mice). Except the highest specific resistance of Colq KO mice which could be explained by the sever growth retardation and muscle weakness of these mice (Bernard et al., 2011; Feng et al., 1999), it is worth noting that all these mice are adapted to the excess of ACh on synaptic ACh receptors and physiologically breathe like WT mice (Fig 1). One can thus assume that, due to the lack of their target in the synapses, ChEIs should not affect the synaptic transmission in the CNS of PRiMA KO mice, and conversely that they should not alter the functioning of the NMJ in Colq KO or AChE1iRR mice. The results obtained allow three main conclusions:

4.1 The respiratory failure induced by ChEIs involves both central and peripheral cholinesterases

When intoxicated with physostigmine, a ChEI that crosses the BBB and therefore acts on both central and peripheral AChE, mutant mice showed a depression of breathing. But in all cases these effects were less marked than in WT mice (Fig 2, 3, 4 and 5). These results support the canonical hypothesis that the respiratory modifications of WT mice involve inhibition of ChEs at both central and peripheral cholinergic synapses. Different doses of physostigmine may help to reveal more effects triggered by ACh.

Among the different changes, the appearance of long “end inspiratory pause” (EIP) accounted for a large part of the reduced frequency in our conditions of exposure to physostigmine or paraoxon. These pauses were almost absent in Colq KO mice in which AChE is normal in CNS. This suggests that the duration of EIP requires the inhibition of peripheral AChE at the NMJ but not in the brain. The duration of these pauses was reduced after physostigmine

poisoning in PRiMA KO and AChE1iRR mice. The differences between AChE1iRR and Colq KO mice support that the duration of EIP is not simply due to the modification of the synaptic transmission at the NMJ that is similarly affected in these mice. In fact, Colq is associated with AChE in several tissues in addition to the skeletal muscles (Taxi and Rieger, 1986), and thus these tissues were probably adapted to AChE deficit in Colq KO but not in AChE1iRR mice. It is also relevant to note that PRiMA anchors AChE and BChE in almost all the peripheral tissues in addition to brain and thus the shorter duration of EIP induced by physostigmine in PRiMA KO mice can be related to the adaptation of peripheral tissues to ChE deficit. Altogether, these results suggest that the long EIP triggered by physostigmine result from the inhibition of cholinesterase in peripheral tissues.

4.2 The end inspiratory pauses which were observed in most exposure may be triggered by activation of afferent pathways

Pauses after inspiration are normal reflexes of mice and are essential to adapt the airflow to the orofacial behavior (i.e. protection of airways, cough swallowing, vocalization…) (Dutschmann et al., 2014; Moore et al., 2014). When mice breathe irritant molecules such as acrolein or cyclohexanone, molecules found in cigarette smoke, long EIP appear in minute. The duration of these pauses is reduced when the mouse breathes simultaneously the irritant molecules and eucalyptol, an agonist of TRMP8, the cold sensitive receptor (Willis et al., 2011). The fact that the long EIP triggered by physostigmine were also reversed by eucalyptol, a counterirritant molecule, suggests that the sensory system is involved in the response to inhibition of ChE.. In airways, non-neuronal ACh has multiple functions and may thus directly or indirectly activate afferent sensory neurons (Kummer and Krasteva-Christ, 2014). Our results thus suggest that the loss of central respiratory drive previously described

during OP exposure (Klein-Rodewald et al., 2011) could be triggered by a direct or indirect action of ACh on afferent sensory neurons in addition to the modifications of cholinergic synaptic transmission in the respiratory centers and at the NMJ.

4.3 Spillover of ACh after inhibition of ChEs could be a major source in the activation of the reflex EIP and exaggerates function of non-neuronal ACh

In our experimental conditions, EIP duration depends on AChE at the NMJ but not directly from the synaptic transmission at the NMJ, and depends on the action of ACh in airways. To link these two observations, we propose that, in addition to the well-known control of the synaptic transmission, a critical function of AChE at the NMJ and presumably in other cholinergic synapses is to prevent the spillover of ACh (Katz and Miledi, 1975). At synaptic level, the spillover of ACh was already described in central cholinergic synapses (Lamotte D'Incamps et al., 2012) and at the NMJ (Petrov et al., 2014) and AChE and BChE seemed both implied in ACh confinement at the synaptic cleft (Petrov et al., 2014). Rats challenged with OPs showed a consecutive flood of ACh in the blood (Stewart, 1952) that may activate distant targets. Thus, the toxicity of ACh would appear when the spillover of ACh from neuron (mainly NMJ) may reach sites where low quantity of ACh, secreted by non-neuronal cells, is used to modulate physiological functions (e.g. inflammation, heart rate, sensory reflexes, etc.) (Grando et al., 2015; Tracey, 2016).

5 Conclusion

The ventilation of mice exposed to ChE inhibitors was strongly altered. We quantified the duration of pauses after inspiration and found 1) the duration of the pauses depends on AChE inhibition at the NMJ and 2) these pauses are reversed by eucalyptol, a counterirritant molecule which suggests that ACh may act as an irritant molecule on sensory system. We propose that physiological hydrolysis of ACh by AChE at the NMJ prevents ACh spillover from the NMJ. Such spillover of ACh when ChEs are inhibited could be critical to ventilation because ACh may activate sensory neurons and trigger reflexes dedicated to respiratory tract protection.

Acknowledgments

Authors were financially supported by the French ministry of Armed Forces (Direction Générale de l'Armement and Service de Santé des Armées) under contracts PDH-2-NRBC-4-C-4204, by AFM-Téléthon (contract 21008) and by CNRS. The authors would like to thank Marc Abitbol, Philippe Ascher and Joseph Kononchik for helpful discussions and their critical reading of the manuscript.

References

Bernard, V., Girard, E., Hrabovska, A., Camp, S., Taylor, P., Plaud, B., Krejci, E., 2011. Distinct localization of collagen Q and PRiMA forms of acetylcholinesterase at the neuromuscular junction. Mol. Cell. Neurosci. 46, 272–281. https://doi.org/10.1016/j.mcn.2010.09.010

Boudinot, E., Bernard, V., Camp, S., Taylor, P., Champagnat, J., Krejci, E., Foutz, A.S., 2009. Influence of differential expression of acetylcholinesterase in brain and muscle on respiration. Respir. Physiol. Neurobiol. 165, 40–48. https://doi.org/10.1016/j.resp.2008.10.003

Camp, S., De Jaco, A., Zhang, L., Marquez, M., De la Torre, B., Taylor, P., 2008. Acetylcholinesterase expression in muscle is specifically controlled by a promoter-selective enhancesome in the first intron. J. Neurosci. Off. J. Soc. Neurosci. 28, 2459–2470. https://doi.org/10.1523/JNEUROSCI.4600-07.2008

Camp, S., Zhang, L., Krejci, E., Dobbertin, A., Bernard, V., Girard, E., Duysen, E.G., Lockridge, O., De Jaco, A., Taylor, P., 2010. Contributions of selective knockout studies to understanding cholinesterase disposition and function. Chem. Biol. Interact. 187, 72–77. https://doi.org/10.1016/j.cbi.2010.02.008

Cannard, K., 2006. The acute treatment of nerve agent exposure. J. Neurol. Sci., Terrorism for the Neurologist 249, 86–94. https://doi.org/10.1016/j.jns.2006.06.008

Chatonnet, F., Boudinot, É., Chatonnet, A., Taysse, L., Daulon, S., Champagnat, J., Foutz, A.S., 2003. Respiratory survival mechanisms in acetylcholinesterase knockout mouse. Eur. J. Neurosci. 18, 1419–1427. https://doi.org/10.1046/j.1460-9568.2003.02867.x

Dobbertin, A., Hrabovska, A., Dembele, K., Camp, S., Taylor, P., Krejci, E., Bernard, V., 2009. Targeting of acetylcholinesterase in neurons in vivo: a dual processing function for the proline-rich membrane anchor subunit and the attachment domain on the catalytic subunit. J. Neurosci. 29, 4519–4530. https://doi.org/10.1523/JNEUROSCI.3863-08.2009

Dolgin, E., 2013. Syrian gas attack reinforces need for better anti-sarin drugs. Nat. Med. 19, 1194–1195. https://doi.org/10.1038/nm1013-1194

Dutschmann, M., Jones, S.E., Subramanian, H.H., Stanic, D., Bautista, T.G., 2014. Chapter 7 - The physiological significance of postinspiration in respiratory control, in: Gert Holstege, C.M.B. and H.H.S. (Ed.), Progress in Brain Research, Breathing, Emotion and Evolution. Elsevier, pp. 113–130.

Duysen, E.G., Li, B., Xie, W., Schopfer, L.M., Anderson, R.S., Broomfield, C.A., Lockridge, O., 2001. Evidence for nonacetylcholinesterase targets of organophosphorus nerve agent: supersensitivity of acetylcholinesterase knockout mouse to VX lethality. J. Pharmacol. Exp. Ther. 299, 528–535.

Duysen, E.G., Stribley, J.A., Fry, D.L., Hinrichs, S.H., Lockridge, O., 2002. Rescue of the acetylcholinesterase knockout mouse by feeding a liquid diet; phenotype of the adult acetylcholinesterase deficient mouse. Brain Res. Dev. Brain Res. 137, 43–54.

Eddleston, M., 2019. Novel Clinical Toxicology and Pharmacology of Organophosphorus Insecticide Self-Poisoning. Annu. Rev. Pharmacol. Toxicol. 59, null. https://doi.org/10.1146/annurev-pharmtox-010818-021842

Farar, V., Mohr, F., Legrand, M., Lamotte d'Incamps, B., Cendelin, J., Leroy, J., Abitbol, M., Bernard, V., Baud, F., Fournet, V., Houze, P., Klein, J., Plaud, B., Tuma, J.,

Zimmermann, M., Ascher, P., Hrabovska, A., Myslivecek, J., Krejci, E., 2012. Near-complete adaptation of the PRiMA knockout to the lack of central acetylcholinesterase. J. Neurochem. 122, 1065–1080. https://doi.org/10.1111/j.1471-4159.2012.07856.x

Feng, G., Krejci, E., Molgo, J., Cunningham, J.M., Massoulié, J., Sanes, J.R., 1999. Genetic analysis of collagen Q: roles in acetylcholinesterase and butyrylcholinesterase assembly and in synaptic structure and function. J. Cell Biol. 144, 1349–1360.

Grando, S.A., Kawashima, K., Kirkpatrick, C.J., Kummer, W., Wessler, I., 2015. Recent progress in revealing the biological and medical significance of the non-neuronal cholinergic system. Int. Immunopharmacol. 29, 1–7. https://doi.org/10.1016/j.intimp.2015.08.023

Ha, M.A., Smith, G.J., Cichocki, J.A., Fan, L., Liu, Y.-S., Caceres, A.I., Jordt, S.E., Morris, J.B., 2015. Menthol Attenuates Respiratory Irritation and Elevates Blood Cotinine in Cigarette Smoke Exposed Mice. PLoS ONE 10, e0117128. https://doi.org/10.1371/journal.pone.0117128

Hartmann, J., Kiewert, C., Duysen, E.G., Lockridge, O., Greig, N.H., Klein, J., 2007. Excessive hippocampal acetylcholine levels in acetylcholinesterase-deficient mice are moderated by butyrylcholinesterase activity. J. Neurochem. 100, 1421–1429. https://doi.org/10.1111/j.1471-4159.2006.04347.x

Hoymann, H.G., 2012. Lung function measurements in rodents in safety pharmacology studies. Pharm. Med. Outcomes Res. 3, 156. https://doi.org/10.3389/fphar.2012.00156

Hulse, E.J., Davies, J.O., Simpson, A.J., Sciuto, A.M., Eddleston, M., 2014. Respiratory Complications of Organophosphorus Nerve Agent and Insecticide Poisoning - Implications for Respiratory and Critical Care. Am. J. Respir. Crit. Care Med. https://doi.org/10.1164/rccm.201406-1150CI

Katz, B., Miledi, R., 1975. The nature of the prolonged endplate depolarization in anti-esterase treated muscle. Proc. R. Soc. Lond. Ser. B Contain. Pap. Biol. Character R. Soc. G. B. 192, 27–38.

Klein-Rodewald, T., Seeger, T., Dutschmann, M., Worek, F., Mörschel, M., 2011. Central respiratory effects on motor nerve activities after organophosphate exposure in a working heart brainstem preparation of the rat. Toxicol. Lett., Selected papers from the 13th Medical Chemical Defence Conference 2011: New Developments in the treatment of intoxications by chemical warfare agents with focus on neurotoxic agents 206, 94–99. https://doi.org/10.1016/j.toxlet.2011.07.005

Kummer, W., Krasteva-Christ, G., 2014. Non-neuronal cholinergic airway epithelium biology. Curr. Opin. Pharmacol., Respiratory • Musculoskeletal 16, 43–49. https://doi.org/10.1016/j.coph.2014.03.001

Lamotte D'Incamps, B., Krejci, E., Ascher, P., 2012. Mechanisms Shaping the Slow Nicotinic Synaptic Current at the Motoneuron–Renshaw Cell Synapse. J. Neurosci. 32, 8413–8423. https://doi.org/10.1523/JNEUROSCI.0181-12.2012

Minic, J., Chatonnet, A., Krejci, E., Molgó, J., 2003. Butyrylcholinesterase and acetylcholinesterase activity and quantal transmitter release at normal and acetylcholinesterase knockout mouse neuromuscular junctions. Br. J. Pharmacol. 138, 177–187. https://doi.org/10.1038/sj.bjp.0705010

Moore, J.D., Kleinfeld, D., Wang, F., 2014. How the brainstem controls orofacial behaviors comprised of rhythmic actions. Trends Neurosci. 37, 370–380. https://doi.org/10.1016/j.tins.2014.05.001

Pennock, B.E., Cox, C.P., Rogers, R.M., Cain, W.A., Wells, J.H., 1979. A noninvasive technique for measurement of changes in specific airway resistance. J. Appl. Physiol. 46, 399–406.

Petrov, K.A., Girard, E., Nikitashina, A.D., Colasante, C., Bernard, V., Nurullin, L., Leroy, J., Samigullin, D., Colak, O., Nikolsky, E., Plaud, B., Krejci, E., 2014. Schwann Cells Sense and Control Acetylcholine Spillover at the Neuromuscular Junction by α7 Nicotinic Receptors and Butyrylcholinesterase. J. Neurosci. 34, 11870–11883. https://doi.org/10.1523/JNEUROSCI.0329-14.2014

Shaffo, F. C., Grodzki, A. C., Fryer, A. D., & Lein, P. J. 2018. Mechanisms of organophosphorus pesticide toxicity in the context of airway hyperreactivity and asthma. American Journal of Physiology-Lung Cellular and Molecular Physiology, 315(4), L485-L501.

Stewart, W. C., 1952. Accumulation of acetylcholine in brain and blood of animals poisoned with cholinesterase inhibitors. British journal of pharmacology and chemotherapy, 7(2), 270-276.

Stone, R., 2018a. Chemical martyrs. American Association for the Advancement of Science.

Stone, R., 2018b. How to defeat a nerve agent. American Association for the Advancement of Science.

Taxi, J., Rieger, F., 1986. Molecular forms of acetylcholinesterase in mammalian smooth muscles. Biol. Cell Auspices Eur. Cell Biol. Organ. 57, 23–32.

Tracey, K.J., 2016. Reflexes in Immunity. Cell 164, 343–344. https://doi.org/10.1016/j.cell.2016.01.018

Willis, D.N., Liu, B., Ha, M.A., Jordt, S.-E., Morris, J.B., 2011. Menthol attenuates respiratory irritation responses to multiple cigarette smoke irritants. FASEB J. 25, 4434–4444. https://doi.org/10.1096/fj.11-188383

Xie, W., Stribley, J.A., Chatonnet, A., Wilder, P.J., Rizzino, A., McComb, R.D., Taylor, P., Hinrichs, S.H., Lockridge, O., 2000. Postnatal developmental delay and supersensitivity to organophosphate in gene-targeted mice lacking acetylcholinesterase. J. Pharmacol. Exp. Ther. 293, 896–902.

Legends

Fig 1. Physiological breathing ventilation of mice with severe deficit in ChE.

(A) Schematic presentation of the double chamber plethysmography device; pnt (pneumotachographs) dpt (differential pressure transducer) (upper part). The nasal (left) and thoracic (right) airflow recorded, opposite nasal signal and thoracic signal have been overlaid in the central diagram (inspiration downward in yellow strip, expiration upward in purple strip) (lower part). (B) Representative example of thorax flow recorded (10 seconds): WT (orange), PRiMA KO (violet), AChE1iRR (olive) and Colq KO (green) mice at least 13min after a subcutaneous injection of vehicle (DMSO diluted into saline solution). (C) The respiratory frequency, the inspiratory time, the expiratory time and the specific airways resistance of breathing of four strains of mice (WT, PRiMA KO, AChE1iRR and Colq KO mice) are represented in box charts (with percentile 25 and 75). Statistical comparisons (one way ANOVA followed by Tukey posthoc test) were carried out between WT (orange, n=8), PRiMA KO (violet, n=8), AChE1iRR (olive, n=8) and Colq KO (green, n=8) mice. P-values of less than 0.05 were considered as significant (* for $p<0.05$, ** for $p<0.01$, *** for $p<0.001$).

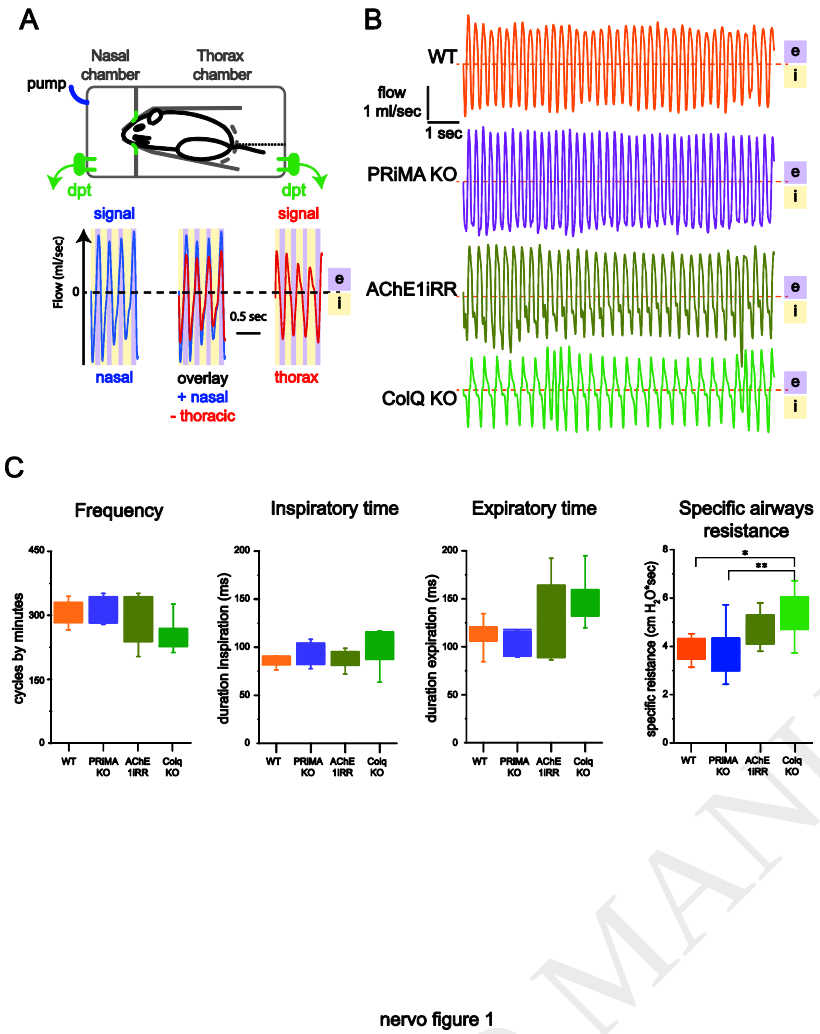

nervo figure 1

Fig 2. Impairment of ventilation of WT mice after administration of paraoxon, physostigmine or pyridostigmine.

(A) Representative examples of breathing pattern of WT mouse, the thoracic flow before injection (grey line) was overlaid by the thoracic flow after subcutaneous injection of vehicle (orange line) or paraoxon (green line) or physostigmine (blue line) or pyridostigmine (red line). (B) Time course of respiratory frequency (cpm) (right) and duration of end inspiratory pause (ms) (left) of WT mice before (yellow zone) and after subcutaneous injection of vehicle (orange, n=8), paraoxon (green, n=8), physostigmine (blue, n=8) or pyridostigmine (red,

n=8). Data are represented as the 1 minute mean±SD. (C) Statistical comparisons (one-way ANOVA followed by Tukey posthoc test) on the respiratory frequency, the inspiratory time, the end inspiratory pause and the specific airways resistance of breathing of WT mice were carried out between control group (orange, n=8), paraoxon (green, n=8), physostigmine (blue, n=8) and pyridostigmine (red, n=8). Data are expressed in percentage of variation compared to the same parameters before injection, or mean value after injection. Data are represented in box charts (with percentile 25 and 75). P-values of less than 0.05 were considered as significant (* for p<0.05, ** for p<0.01, *** for p<0.001).

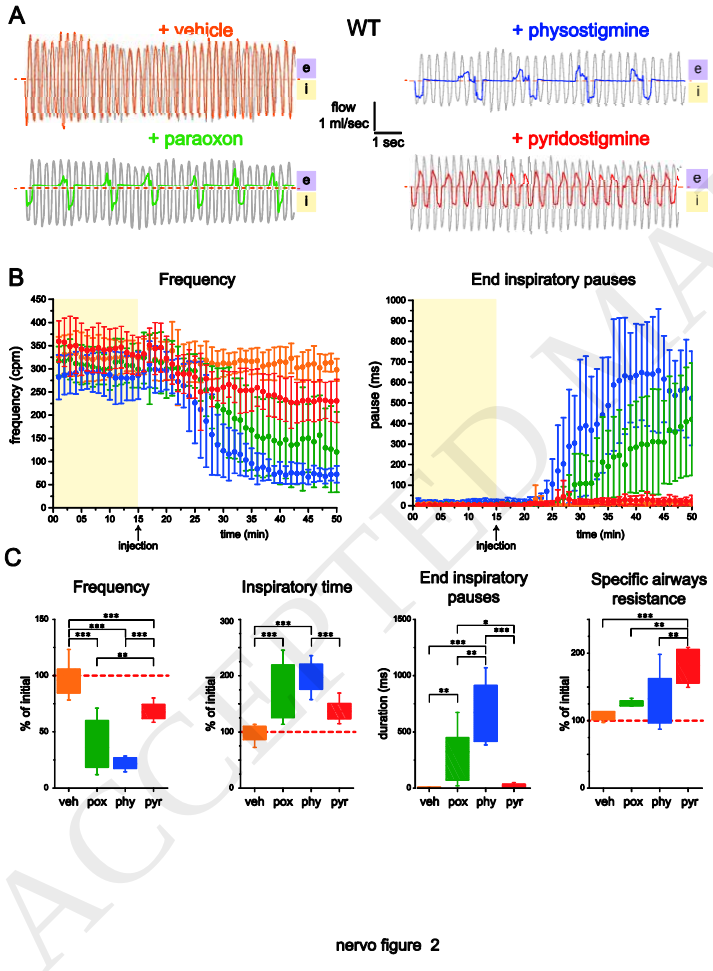

nervo figure 2

Fig 3. Impairment of ventilation of PRiMA KO mice after administration of physostigmine or pyridostigmine.

(A) Representative example of breathing pattern of a PRiMA KO mouse, the thoracic flow before injection (grey) was overlaid by the thoracic flow after subcutaneous injection of vehicle (orange) or physostigmine (blue) or pyridostigmine (red). (B) Time course of respiratory frequency (cpm) (right) and duration of end inspiratory pause (ms) (left) of PRiMA KO mice before (yellow zone) and after subcutaneous injection of vehicle (orange, n=8), physostigmine (blue, n=8) or pyridostigmine (red, n=9) (left). Data are represented as the 1 minute mean±SD. (C) Statistical comparisons (one way ANOVA followed by Tukey posthoc test) on the respiratory frequency, the inspiratory time, the end inspiratory pauses and the specific airways resistance of breathing of PRiMA KO mice were carried out between control group (orange, n=8), physostigmine (blue, n=8) and pyridostigmine (red). Data are expressed in percentage of variation compared to the same parameters before injection, or mean value after injection. Data are represented in box charts (with percentile 25 and 75). P-values of less than 0.05 were considered as significant (* for $p<0.05$, ** for $p<0.01$, *** for $p<0.001$).

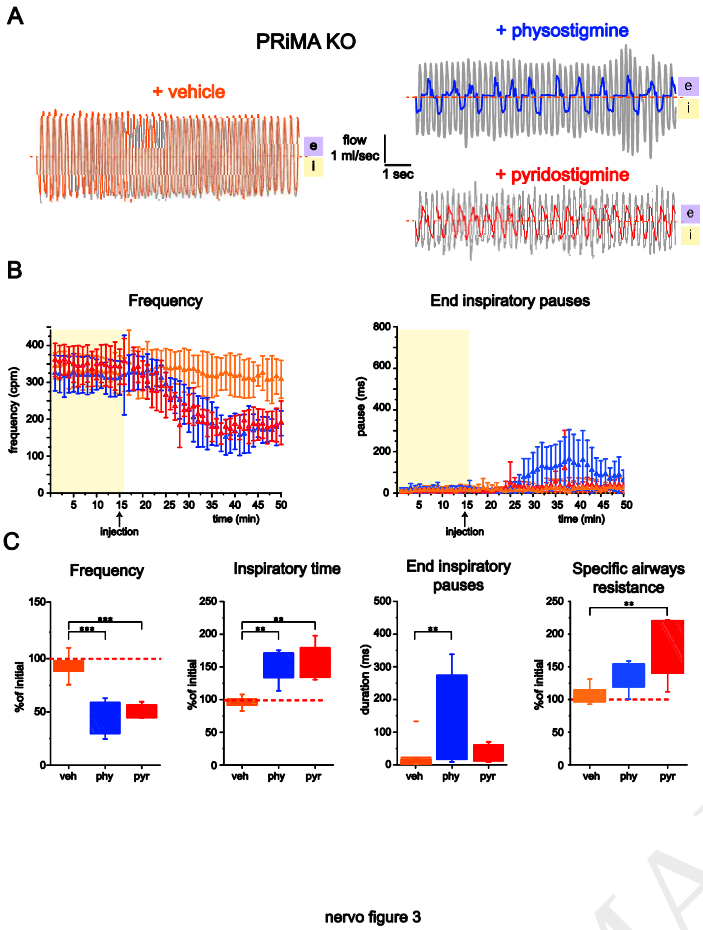

Fig 4. Deficit of AChE at the NMJ prevents acute depression of respiration by physostigmine.

(A) Representative example of breathing pattern Colq KO mice, the thoracic flow before injection (grey) was overlaid by the thoracic flow after subcutaneous injection of physostigmine (blue). (B) Time course of respiratory frequency (cpm) (right) and duration of end inspiratory pause (ms) (left) of WT (grey, n=8) and Colq KO (green, n=8) mice before (yellow zone) and after subcutaneous injection of physostigmine. Data are represented as the 1 minute mean±SD. (C) Statistical comparisons (one way ANOVA followed by Tukey posthoc test) on the respiratory frequency, the inspiratory time, the end inspiratory pauses and the specific airways resistance of breathing were carried out between WT (grey, n=8) and

Colq KO (green, n=8) mice. Data are expressed in percentage of variation compared to the same parameters before injection, or mean value after injection. Data are represented in box charts (with percentile 25 and 75). P-values of less than 0.05 were considered as significant (* for p<0.05, ** for p<0.01, *** for p<0.001).

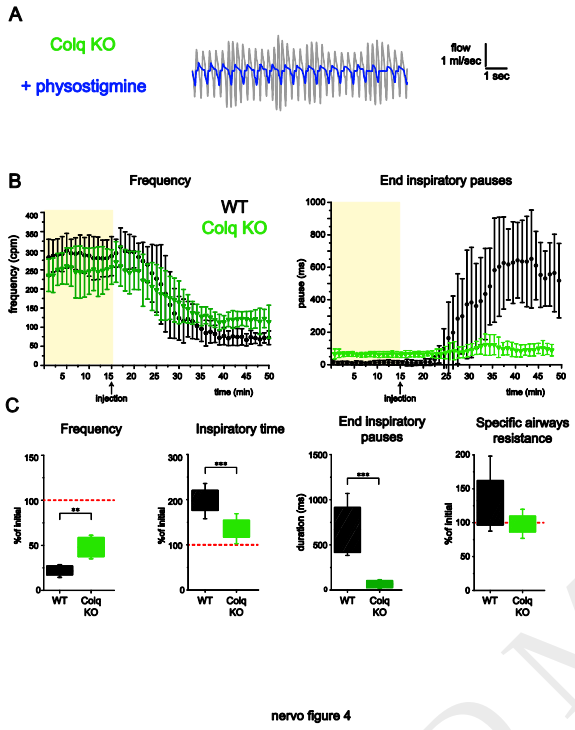

Fig 5. Impairment of ventilation of AChE1iRR mice after administration of physostigmine or pyridostigmine.

(A) Representative example of breathing pattern of a AChE1iRR mouse, the thoracic flow before injection (grey) was overlaid by the thoracic flow after subcutaneous injection of vehicle (orange) or physostigmine (blue) or pyridostigmine (red). (B) Time course of respiratory frequency (cpm) (right) and duration of end inspiratory pause (ms) (left) of PRiMA KO mice before (yellow zone) and after subcutaneous injection of vehicle (orange, n=8), physostigmine (blue, n=8) or pyridostigmine (red, n=9) (left). Data are represented as

the 1 minute mean±SD. (C) Statistical comparisons (one way ANOVA followed by Tukey posthoc test) on the respiratory frequency, the inspiratory time, the end inspiratory pauses and the specific airways resistance of breathing of AChE1iRR mice were carried out between control group (orange), physostigmine (blue) and pyridostigmine (red). Data are expressed in percentage of variation compared to the same parameters before injection, or mean value after injection. Data are represented in box charts (with percentile 25 and 75). P-values of less than 0.05 were considered as significant (* for p<0.05, ** for p<0.01, *** for p<0.001).

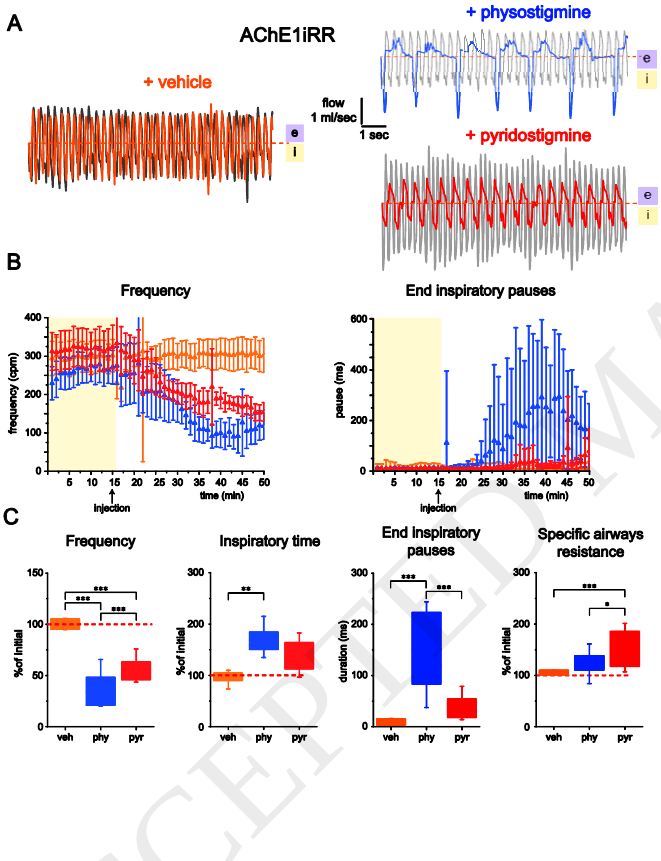

nervo figure 5

Fig 6. Eucalyptol reversed the long pause triggered by physostigmine in WT mice.

(A) Representative examples of breathing patterns. The thoracic flow before injection or instillation was presented as grey line. Left pattern, the thoracic flow after two instillations of eucalyptol alone was presented. Right patterns the thoracic flow after subcutaneous injection of physostigmine alone (blue line) or treated by eucalyptol instillations (green line). (B) Time course of respiratory frequency (cpm) (right) and duration of end inspiratory pause (ms) (left) before (yellow zone) and after subcutaneous injection of physostigmine (blue, n=8) and physostigmine + eucalyptol treatments (green, n=8). Data are represented as the 1 minute mean±SD. Eucalyptol has been instilled twice as noted by green arrows. (C) Statistical comparisons (one way ANOVA followed by Tukey posthoc test) on the respiratory frequency, the inspiratory time, the end inspiratory pauses and the specific airways resistance of breathing of WT mice were carried out between control group (grey, n=8), eucalyptol alone (green, n=5), physostigmine alone (blue, n=8) and physostigmine + eucalyptol treatment (green, n=8). Data are expressed in percentage of variation compared to the same parameters before injection, or mean value after injection. Data are represented in box charts (with percentile 25 and 75).. P-values of less than 0.05 were considered as significant (* for $p<0.05$, ** for $p<0.01$, *** for $p<0.001$).

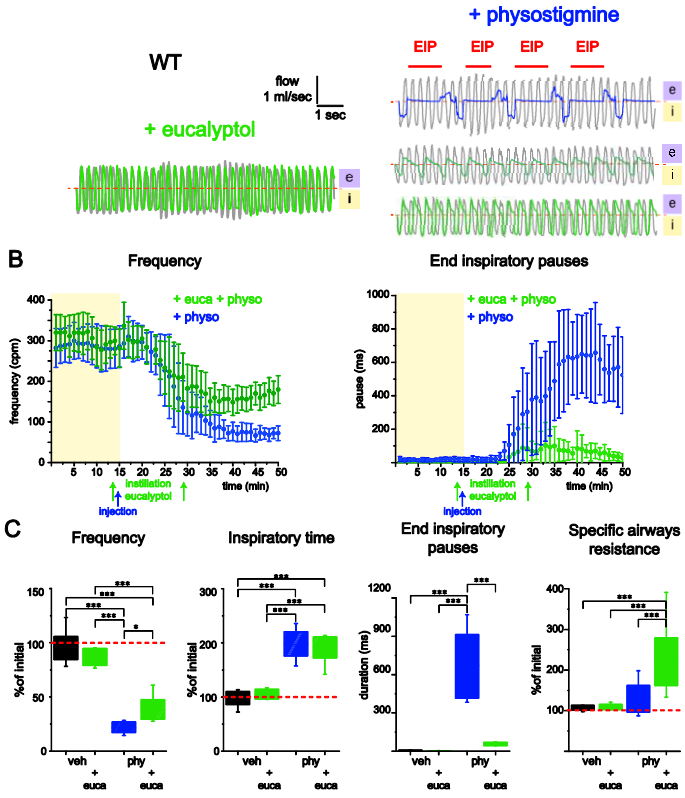

nervo figure 6